

# Impact of Renal Denervation on Atrial Arrhythmogenic Substrate in Ischemic Model of Heart Failure

Shinya Yamada, MD;\* Man-Cai Fong, MD;\* Ya-Wen Hsiao, PhD; Shih-Lin Chang, MD; Yung-Nan Tsai, Msc; Li-Wei Lo, MD; Tze-Fan Chao, MD; Yenn-Jiang Lin, MD; Yu-Feng Hu, MD; Fa-Po Chung, MD; Jo-Nan Liao, MD; Yao-Ting Chang, MD; Hsing-Yuan Li, MD; Satoshi Higa, MD; Shih-Ann Chen, MD

**Background**—Myocardial infarction increases the risk of heart failure (HF) and atrial fibrillation. Renal denervation (RDN) might suppress the development of atrial remodeling. This study aimed to elucidate the molecular mechanism of RDN in the suppression of atrial fibrillation in a HF model after myocardial infarction.

**Methods and Results**—HF rabbits were created 4 weeks after coronary ligation. Rabbits were classified into 3 groups: normal control (n=10), HF (n=10), and HF-RDN (n=6). Surgical and chemical RDN were approached through midabdominal incisions in HF-RDN. Left anterior descending coronary artery in HF and HF-RDN was ligated to create myocardial infarction. After electrophysiological study, the rabbits were euthanized and the left atrial appendage was harvested for real-time polymerase chain reaction analysis and Trichrome stain. Left atrial dimension and left ventricular mass were smaller in HF-RDN by echocardiography compared with HF. Attenuated atrial fibrosis and tyrosine hydroxylase levels were observed in HF-RDN compared with HF. The mRNA expressions of Cav1.2, Nav1.5, Kir2.1, KvLQT1, phosphoinositide 3-kinase, AKT, and endothelial nitric oxide synthase in HF-RDN were significantly higher compared with HF. The effective refractory period and action potential duration of HF-RDN were significantly shorter compared with HF. Decreased atrial fibrillation inducibility was noted in HF-RDN compared with HF (50% versus 100%,  $P<0.05$ ).

**Conclusions**—RDN reversed atrial electrical and structural remodeling, and suppressed the atrial fibrillation inducibility in an ischemic HF model. The beneficial effect of RDN may be related to prevention of the downregulation of the phosphoinositide 3-kinase/AKT/endothelial nitric oxide synthase signaling pathway. (*J Am Heart Assoc.* 2018;7:e007312. DOI: 10.1161/JAHA.117.007312.)

**Key Words:** apoptosis • atrial arrhythmogenic substrates • atrial fibrillation • PI3K/AKT/eNOS signaling • renal denervation

Ischemic cardiomyopathy is a major cause of heart failure (HF), which can lead to damage of cardiomyocytes, fibrosis, and cardiac hypertrophy and dilatation.<sup>1,2</sup> In patients with myocardial infarction (MI), atrial fibrillation (AF) is considered to be the most frequently occurring supraventricular tachycardia with an incidence of 6% to 21%.<sup>3,4</sup> The patients with MI who developed AF are at a greater risk for HF-related hospitalization and mortality than those without

AF.<sup>3,5</sup> In an ischemic HF rabbit model, structural and electrical remodeling in the atrium were observed, which was associated with high AF inducibility.<sup>6–8</sup> The activity of the phosphoinositide 3-kinase (PI3K)/AKT/endothelial nitric oxide synthase (eNOS) signaling pathway plays an important role in the inhibition of pathologic signaling cascades in AF.<sup>6</sup>

Renal denervation (RDN) has been demonstrated to attenuate sympathetic outflow via the brain to the heart as

From the Division of Cardiology, Department of Medicine (S.Y., Y.W.H., S.-L.C., Y.-N.T., L.W.L., T.-F.C., Y.-J.L., Y.-F.H., F.-P.C., J.-N.L., Y.-T.C., H.-Y.L., S.-A.C.), Department of Pediatrics (H.-Y.L.), Taipei Veterans General Hospital, Taipei, Taiwan; Department of Cardiovascular Medicine, Fukushima Medical University, Fukushima, Japan (S.Y.); Heart Center, Cheng Hsin General Hospital, Taipei, Taiwan (M.-C.F.); Institute of Clinical Medicine, and Cardiovascular Research Institute, National Yang-Ming University, Taipei, Taiwan (S.-L.C., Y.-N.T., L.-W.L., T.-F.C., Y.-J.L., Y.-F.H., F.-P.C., J.-N.L., Y.-T.C., S.-A.C.); Division of Cardiology, Department of Medicine, National Defense Medical Center, Taipei, Taiwan (M.-C.F.); Division of Cardiovascular Medicine, Cardiac Electrophysiology and Pacing Laboratory, Makimato Central Hospital, Okinawa, Japan (S.H.).

\*Dr Yamada and Dr Fong contributed equally to this work.

**Correspondence to:** Shih-Lin Chang, MD, PhD, Division of Cardiology, Department of Medicine, Taipei Veterans General Hospital, No. 201, Sec. 2, Shih-Pai Rd, Taipei, Taiwan. E-mail: slchang4@vghtpe.gov.tw

Received August 4, 2017; accepted November 28, 2017.

© 2018 The Authors. Published on behalf of the American Heart Association, Inc., by Wiley. This is an open access article under the terms of the Creative Commons Attribution-NonCommercial License, which permits use, distribution and reproduction in any medium, provided the original work is properly cited and is not used for commercial purposes.

## Clinical Perspective

### What Is New?

- The extension of atrial fibrosis and structural remodeling in rabbits with ischemic heart failure (HF) was significantly suppressed in rabbits with HF-renal denervation.
- The beneficial effect of renal denervation on cardiac remodeling may be related to prevention of the downregulation of phosphoinositide 3-kinase/AKT/endothelial nitric oxide synthase signaling pathway in a HF model.

### What Are the Clinical Implications?

- Renal denervation regulates the progression of atrial electrical and structural remodeling, and suppresses the atrial fibrillation inducibility in an ischemic HF model.
- The combination of atrial fibrillation and HF is associated with a higher risk of mortality. From our study, renal denervation might be an alternative therapeutic strategy in selected patients, particularly when medical therapy for HF with atrial fibrillation is ineffective or suboptimal.

well as decreasing systemic catecholamine excretion.<sup>9</sup> Although the Symplicity HTN-3 trial failed to demonstrate a beneficial result of RDN in patients with resistant hypertension,<sup>10</sup> several studies showed that RDN might have great potential in the treatment of cardiovascular diseases including HF<sup>11</sup> and AF,<sup>12</sup> beyond the changes of blood pressure. We recently reported that atrial arrhythmogenesis was regulated by RDN, mostly through suppressing structural remodeling in rapid ventricular 4-week pacing models.<sup>13</sup> However, in that study, ionic channel remodeling was not observed in pacing HF models because the severity of cardiac remodeling directly correlates with the rate and duration of pacing.<sup>14</sup> Therefore, this study aimed to investigate whether RDN can protect the atrium from structural and electrical remodeling in an ischemic HF model. Another goal was to elucidate the beneficial effect of RDN on the molecular mechanisms in the suppression of AF in an ischemic HF model.

## Methods

We will not make the data, methods used in the analysis, and materials used to conduct the research available to any researcher for purposes of reproducing the results or replicating the procedure.

## Animal Preparation

The present study was approved by the Institutional Animal Care and Ethics Committee of the Taipei Veterans General Hospital (IACUC: 2014-120) and was in strict accordance

with the US National Institutes of Health or European Commission guidelines. All surgical procedures were performed with the animals under general anesthesia. All efforts were made to minimize suffering of the animals. A total of 32 male New Zealand white rabbits (weight 2–3 kg, from Shulin Breeding facility, New Taipei, Taiwan) at 12 weeks of age were used. One animal per cage (530×630×320 mm) was housed in a temperature- (22–25°C) and humidity (50%–70%)-regulated room with a maintained light–dark cycle (12 hours light from 7:00 AM to 7:00 PM and 12 hours dark from 7:00 PM to 7:00 AM), and unlimited access to food (Laboratory Rabbit Diet 5326 HF; PMI, Richmond, IN) and water.

## HF Model by Coronary Ligation

The procedure for the creation of the HF rabbit model by myocardial ischemia was modified from a previous study.<sup>15</sup> Repeated injections of Zoletil 50 (10 mg/kg) and xylazine (5 mg/kg) were administered as required to maintain a deep level of anesthesia. The rabbits were intubated with an endotracheal tube and mechanically ventilated. A left thoracotomy was performed through the fourth intercostal space. The major ventricular branch of the left coronary artery was ligated halfway between its origin and the cardiac apex. Successful ligation was confirmed by the presence of large homogeneous cyanosis with bulging and ST-segment changes in the surface ECG signal. A prophylactic antibiotic agent was given as intramuscular injection for 48 hours. HF status was confirmed by the presentation of signs of ascites, edema, drowsiness, and dyspnea, which were compatible with experimental and clinical HF 4 weeks after coronary ligation.<sup>6–8</sup>

## Surgical and Chemical Rabbit RDN Model

RDN was performed at the time of coronary ligation. By using the same anesthesia method, both kidneys were approached through midabdominal incision. This chemical RDN has been reported before.<sup>13,16</sup> In brief, the rabbit underwent fasting for 1 night before the surgery. Bilateral kidneys were surgically denervated by cutting all visible nerves in the area of the renal hilus (surgical RDN) and by stripping ≈1 cm of the adventitia from the renal artery. The area was then moistened with a 20% phenol solution for 10 to 15 minutes (chemical RDN). Following RDN, the animals were allowed to re-equilibrate for 1 hour and the abdomen was closed layer by layer with suture and bleeding was checked.

## Echocardiography

Two-dimensional echocardiography was performed 4 weeks after intervention in all rabbits (MicroMaxx, SonoSite Inc,

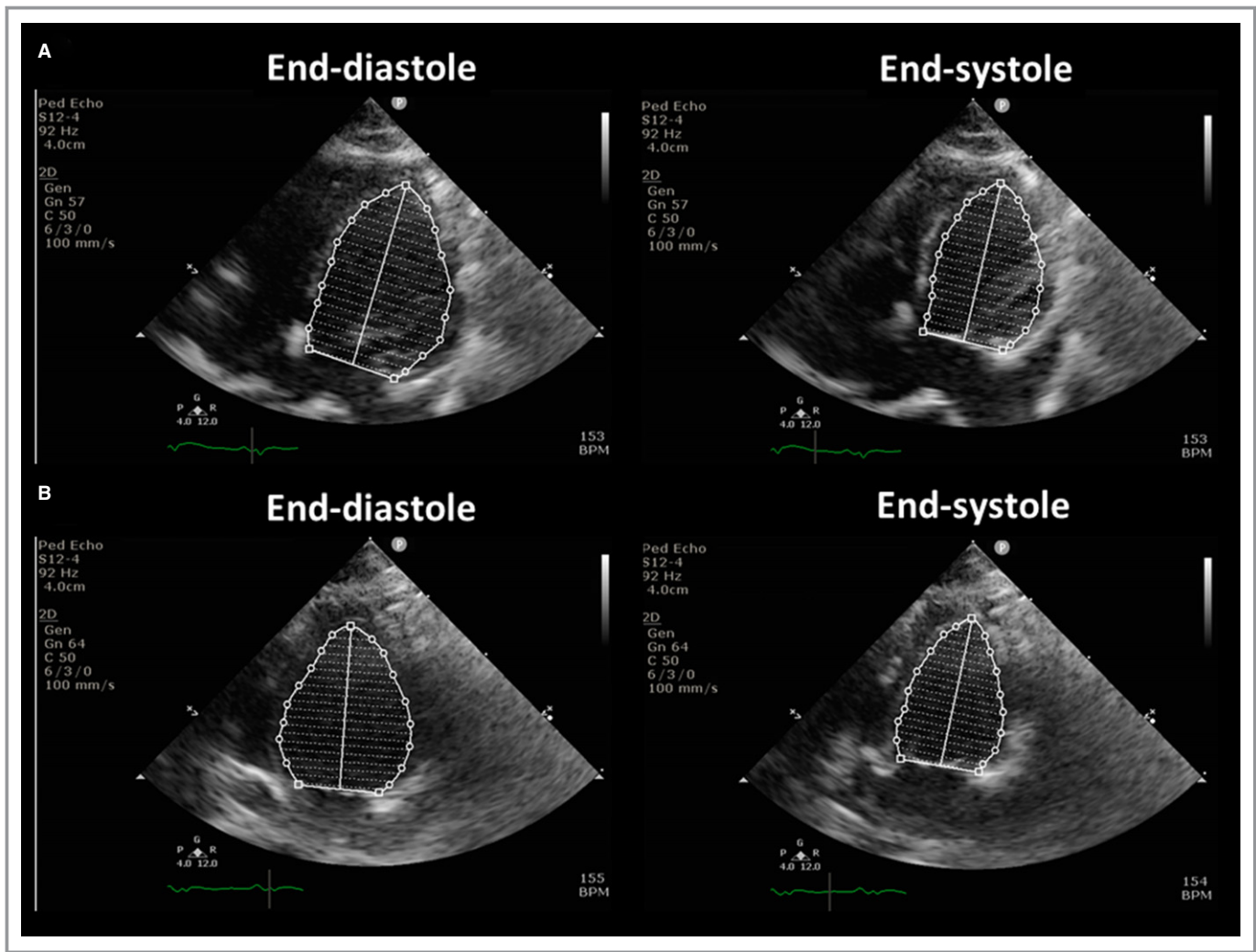


**Figure 1.** The calculation of left ventricular ejection fraction. Left ventricular ejection fraction was calculated using the biplane Simpson method. See text for details. A, The apical 4-chamber views at the end of diastole (left panel) and systole (right panel). B, The apical 2-chamber views at the end of diastole (left panel) and systole (right panel). BPM indicates beats per minute.

Bothell, WA). Left atrial (LA) diameter, left ventricular internal dimensions at diastole and systole, left ventricular fractional shortening, and left ventricular ejection fraction and left ventricular (LV) mass were chosen for analysis. Left ventricular fractional shortening (left ventricular internal dimensions at diastole and left ventricular internal dimensions at systole) was measured using the M mode in the parasternal short-axis view. LA diameter was measured at the end systole in the parasternal long-axis view. Left ventricular ejection fraction was calculated using the biplane Simpson method. LV end-diastolic and end-systolic volumes were measured using the biplane method of discs' summation (modified Simpson's rule) using 2-dimensional images from both the apical 4- and 2-chamber views (Figure 1A and 1B). The LV mass was measured by M-mode echocardiography with the use of the Devereux formula.<sup>17</sup>

### Biochemical Study

Blood samples were collected from the central auricular artery of the rabbits after coronary ligation followed by observation for 4 weeks. The plasma was obtained by centrifuging the blood at 1710 g for 10 minutes at 4°C, and then the levels of plasma renin activity, renin, and aldosterone were examined.

### Experimental Procedures

The rabbits were randomized to 4 groups:

1. Normal control group (n=10): The rabbits without coronary ligation or RDN.
2. HF group (n=10): The rabbits received coronary ligation followed by observation for 4 weeks before experiment.
3. HF-RDN group (n=6): The rabbits received both coronary ligation and bilateral RDNs.

4. RDN sham group (n=6): HF rabbits with open abdomen surgery and without RDN.

### General preparation

On the day of experiment, a warming blanket was used for rabbits to maintain the body temperature. An intravenous line was set up for the medication and fluid supplement. All rabbits were anesthetized with an intraperitoneal injection of sodium pentobarbital (40 mg/kg). They were artificially ventilated through a cuffed endotracheal tube by a constant-volume cycled respirator with room air or oxygen as needed. The rabbit was placed in the supine position. A midthoracotomy was performed and the muscle was dissected with careful checking for bleeding during the procedure until the exposure of the mediastinal space. The pericardium was then incised to expose the whole heart completely.

### Conventional electrophysiology study

The surface ECG and intracardiac electrograms were recorded continuously using a computer-based digital amplifier/recorder system (Lab System™ PRO EP Recording System, Bard, MA) with sampling rate of 2 kHz. Monophasic action potentials (MAPs) were recorded during sinus rhythm from the epicardium by means of a mapping catheter at the left atrial appendage (LAA).<sup>6–8</sup> The MAPs were filtered from 0.05 to 500 Hz. The signals were digitized at 1 kHz to 16-bit resolution and exported from the recorder (Bard Pro, Billerica, MA) for an analysis using custom PC software written in Lab View (National Instruments, Austin, TX). The signals with an unstable baseline, noise, or artifact were excluded. In the present study, the criteria of stability for MAP recording was defined as the reproducible and consistent baseline amplitude with a variation of <20% and a stable duration measured at 90% repolarization. Less than 5% of MAP recordings were excluded from analysis. The effective refractory period (ERP) was measured (2 times the diastolic threshold, 2-ms pulse width, and mean of 3 determinations) at basic cycle lengths of 300, 250, and 200 ms with a train of 7 basic (S1) stimuli followed by a premature (S2) stimulus with 2-ms decrements at the 4 sites of interest of the LAA using the contact MAP pacing catheters. The ERP was defined as the longest S1 to S2 interval that failed to produce an action potential. The action potential duration (APD) was measured from the steepest deflection of the slope of phase 0 of the MAP to the time of 90% repolarization (APD<sub>90</sub>). A standardized burst pacing protocol was performed to induce AF.<sup>6</sup> Induced AF with a minimal duration of 1 s was defined as the incidence of sustained AF.<sup>8</sup>

### Tissue harvest

The rabbits were euthanized by exsanguination under anesthesia at the end of the mapping procedure and atrial

myocardium harvested from 3 groups was obtained. Fixation procedure was performed immediately in both 20% formalin and liquid nitrogen to prevent sample degradation. Renal sampling was also performed with kidneys frozen in liquid nitrogen and stored at –80°C to allow adrenaline, nora-adrenaline, and dopamine concentrations to be determined.

### Real-Time Polymerase Chain Reaction

Total RNA was isolated from rabbit LAA tissue with the RNeasy Fibrous Tissue Kit (Qiagen, Valencia, CA) according to the manufacturer's instructions. In the present study, the messenger RNA (mRNA) expressions of Cav1.2, Nav1.5, Kir2.1, KvLQT1, PI3K, AKT, and eNOS were investigated in all rabbits. Complementary DNA (cDNA) was synthesized by PrimeScript™ Reverse Transcriptase (Takara Bio Inc, Kyoto, Japan) using random hexamers from 5.0 µg of total RNA. The resulting cDNA was measured by quantitative real-time polymerase chain reaction (PCR) using the Maxima® SYBR Green quantitative PCR Master Mix (Thermo Scientific Inc, MD) for 40 cycles at an annealing temperature of 55°C with the Step One® real-time PCR system (Applied Biosystems, Carlsbad, CA). Threshold cycles were recorded in all samples for the target and reference gene, glyceraldehyde-3-phosphate dehydrogenase. Melt curve analysis was performed for each run. The relative target gene expression was calculated

**Table 1.** Primer for Real-Time PCR

| Gene   | Primer (5'→3')           | NCBI Accession No. |
|--------|--------------------------|--------------------|
| Cav1.2 | F: GCTCGAGAAAGGAAGTGGTG  | NM_001129846       |
|        | R: GGAAGGGATGGAGAAAGGAG  |                    |
| Nav1.5 | F: CTGGAACATCTTCGACAGCA  | XM_002724008       |
|        | R: GACTTGGCCAGCTTGAAGAC  |                    |
| Kir2.1 | F: CAGACACTCCCCCTGACATT  | NM_001082198       |
|        | R: CCAGAGAAGGAGTCGGTCAG  |                    |
| KvLQT1 | F: ACCACTTCACCGTGTCTCCTC | XM_002723606       |
|        | R: GAACACCACCAGGACGATCT  |                    |
| PI3K   | F: CCTGTGGGAGGAACAACAGT  | XM_002713457       |
|        | R: TGTTCGATGAGCTTTGGTGAG |                    |
| AKT    | F: ATGGCACCTTCATTGGCTAC  | NM_005163          |
|        | R: CCCAGCAGCTTCAGGTAICTC |                    |
| eNOS   | F: CAGCCTCACTCCTGTCTTCC  | AY964103           |
|        | R: GTGGCCTTCACTCTCTTTGC  |                    |
| GAPDH  | F: AGGTCATCCACGACCACTTC  | NM_001082253       |
|        | R: GTGAGTTTCCCGTTCAGCTC  |                    |

eNOS indicates endothelial nitric oxide synthase; NCBI, National Center for Biotechnology Information; PCR, polymerase chain reaction; PI3K, phosphoinositide 3-kinase.

**Table 2.** Echocardiographic Findings 4 Weeks After MI

|                             | Control          | HF                              | HF-RDN           | P Value |
|-----------------------------|------------------|---------------------------------|------------------|---------|
| LA diameter, mm             | 7.2 (6.3–7.4)    | 10.2 (9.4–10.9) * <sup>†</sup>  | 7.7 (7.0–9.4)    | <0.01   |
| LVIDd, mm                   | 13.5 (13.0–14.4) | 17.3 (16.7–18.3) <sup>‡,§</sup> | 12.6 (11.0–12.9) | <0.01   |
| LVIDs, mm                   | 8.5 (8.4–8.6)    | 11.8 (11.1–12.1) * <sup>§</sup> | 8.0 (6.7–9.7)    | <0.01   |
| LV ejection fraction, %     | 70.0 (68.7–74.5) | 40.0 (38.2–42.7) * <sup>§</sup> | 71.0 (58.0–76.0) | <0.01   |
| LV fractional shortening, % | 36.1 (35.0–39.7) | 32.1 (31.4–32.6) *              | 36.4 (27.6–40.7) | 0.03    |
| LV mass, g                  | 3.5 (3.0–3.7)    | 4.8 (4.4–5.6) * <sup>§</sup>    | 3.5 (3.2–3.9)    | <0.01   |

Data are presented as median (interquartile range). HF indicates heart failure; LA, left atrium; LV, left ventricle; LVIDd, left ventricular internal dimension at diastole; LVIDs, left ventricular internal dimension at systole; MI, myocardial infarction; RDN, renal denervation.

\* $P < 0.01$  vs control, <sup>†</sup> $P < 0.05$  vs HF-RDN rabbits, <sup>‡</sup> $P < 0.05$  vs control, and <sup>§</sup> $P < 0.01$  vs HF-RDN rabbits.

as  $\Delta$ threshold cycles, determined by subtracting the threshold cycles of the reference gene from that of the target gene. All reactions were performed in triplicate. Primer sequences for real-time PCR detection are shown in Table 1.

### Western Blot Analysis

Tissues from LAAs isolated were suspended in a lysis buffer. Protein samples were separated on 10% or 15% sodium dodecyl sulfate–polyacrylamide gel electrophoresis and then

transferred to polyvinylidene difluoride membranes (Millipore, Bedford, MA). The membrane was blocked in 5% bovine serum albumin buffer for 1 hour and then incubated with primary antibodies against cleaved caspase 3 (Millipore), and caspase 3 (Thermo Scientific). Proteins were detected by Immobilon Western chemiluminescent horseradish peroxidase substrate (Millipore). In the present study, HF rabbits undergoing coronary artery ligation combined with midabdominal incision surgery (RDN sham,  $n=6$ ) were also assessed in order to evaluate cardiac apoptosis after abdomen surgery.

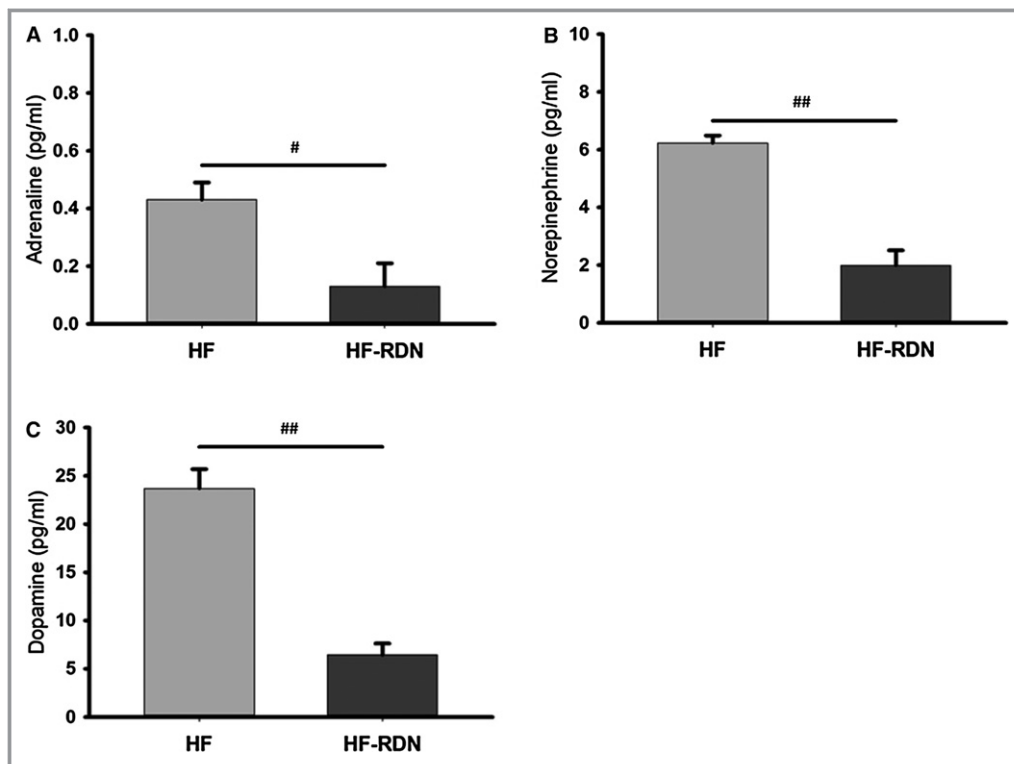


**Figure 2.** Renal tissue catecholamine in left atrial appendage. A, The adrenaline content of renal tissue extracts. B, The norepinephrine content of renal tissue extracts. C, The dopamine content of renal tissue extracts. # $P < 0.05$  and ## $P < 0.01$ . HF indicates heart failure; RDN, renal denervation.

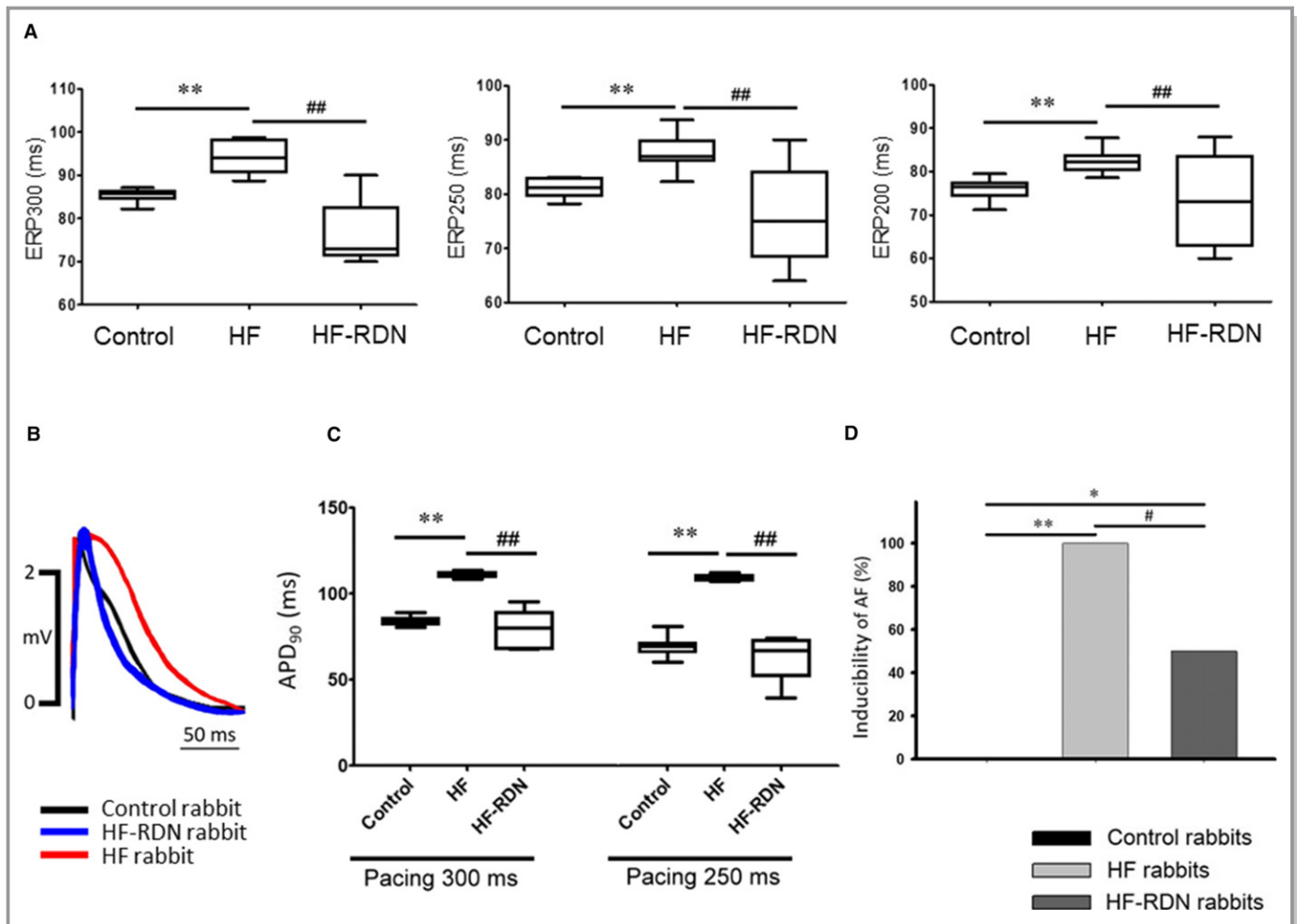


**Figure 3.** Electrophysiology study in LAA. A, ERPs among 3 groups. Left panel shows ERP at basic cycle lengths of 300 ms. Middle panel shows ERP at basic cycle lengths of 250 ms. Right panel shows ERP at basic cycle lengths of 200 ms. B, An example of MAP during a pacing cycle length of 300 ms among 3 groups. C, APD<sub>90</sub> at pacing cycle lengths of 300 and 250 ms. APD<sub>90</sub> indicates the action potential duration measured from the steepest deflection of the slope of phase 0 of the MAP to the time of 90% repolarization. D, Inducibility of AF. \* $P < 0.05$  and \*\* $P < 0.01$  (vs control) and # $P < 0.05$  and ## $P < 0.01$  (vs HF-RDN). AF indicates atrial fibrillation; APD, action potential duration; ERP, effective refractory period; HF, heart failure; LAA, left atrial appendage; MAP, monophasic action potential; RDN, renal denervation.

## Histological Study

LAA samples were collected and fixed in 10% neutral buffered formalin. The samples were then embedded in paraffin and sectioned (4 to 5  $\mu$ m). Preparations were stained with Masson's trichrome stain and examined by light microscopy ( $\times 40$ ) for collagen. The amount of collagen in the area under observation was determined by Image-Pro Plus 6.0 (Media Cybernetics, Bethesda, MD) after digitizing 6 randomly selected fields per section with a slide scanner. Areas containing blood vessels and perivascular interstitial cells were excluded from the analysis. Percentage of fibrosis was calculated as the ratio of the total area of fibrosis to the total area of LAA tissues analyzed. For the immunohistochemistry staining, antibodies for tyrosine hydroxylase were used to stain sympathetic nerves. The cross-sectional areas of the

tyrosine hydroxylase-positive portions of LAA were calculated as a percentage of the total LAA area. In addition, immunohistochemistry staining of transforming growth factor- $\beta$  was also assessed in the myocardial tissue. The cross-sectional areas of the transforming growth factor- $\beta$ -positive portions of LAA were calculated as a percentage of the total LAA area. These areas were determined by Image-Pro Plus 6.0.

## Statistical Analysis

Normally distributed data were reported as mean values  $\pm$  SE. Other not normally distributed data were reported as median and interquartile range. Categorical data were presented as absolute values and percentages. Data variables among the groups (intergroup) were compared with the Kruskal-Wallis test, and if  $P$  was  $< 0.05$ , follow-up comparisons of the

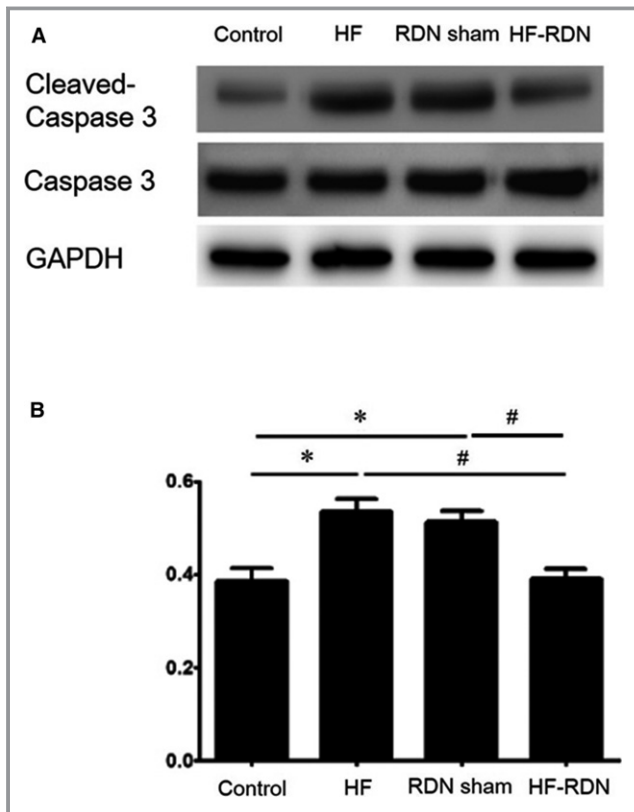


**Figure 4.** Myocardial apoptosis in left atrial appendage. A, Protein expression of cleaved caspase 3 and caspase 3 in each group by Western blot analysis. B, The ratio of cleaved caspase 3 to caspase 3 was evaluated in each group. \* $P < 0.05$  (vs control) and # $P < 0.05$  (vs HF-RDN). RDN sham indicates HF rabbit with open abdomen surgery without RDN. HF indicates heart failure; RDN, renal denervation.

different groups were done with the Dunn's test.  $P < 0.05$  was deemed statistically significant. Analysis was performed by a senior biostatistician using SPSS statistical software (Version 22.0, SPSS Institute Inc, Chicago, IL).

## Results

### Echocardiographic Data and Catecholamine in Kidney Tissue

Echocardiographic findings are shown in Table 2. Although HF rabbits had a lower left ventricular fractional shortening and left ventricular ejection fraction than control rabbits, HF-RDN rabbits showed higher left ventricular fractional shortening and left ventricular ejection fraction compared with HF rabbits. HF rabbits had a greater LA diameter, left ventricular internal dimensions at diastole, left ventricular internal dimensions at systole, and LV mass than those in control rabbits, whereas HF-RDN rabbits revealed smaller LA diameter, left ventricular internal dimensions at diastole, left ventricular internal dimensions at systole, and LV mass as compared with HF rabbits.

The adrenaline, norepinephrine, and dopamine contents of renal tissue extracts were significantly decreased in HF-RDN rabbits compared with those of HF rabbits as shown in Figure 2. There were no significant differences in adrenaline and norepinephrine on the LAA samples between HF rabbits and HF-RDN rabbits (adrenaline,  $0.62 \pm 0.26$  versus  $0.31 \pm 0.13$  pg/mL; norepinephrine,  $4.87 \pm 0.19$  versus  $4.91 \pm 0.03$  pg/mL, respectively).

In biochemical study, there were no significant differences in the levels of plasma renin activity ( $1.00 \pm 0.09$ ,  $1.27 \pm 0.19$  and  $1.77 \pm 0.45$  ng/mL per hour), renin ( $0.19 \pm 0.12$ ,  $0.24 \pm 0.17$  and  $0.44 \pm 0.23$  pg/mL), and aldosterone ( $53.6 \pm 30.6$ ,  $72.6 \pm 38.3$  and  $107.6 \pm 56.0$  pg/mL) among control rabbits, HF rabbits, and HF-RDN rabbits.

### Electrophysiology Study and the Inducibility of AF

Figure 3A shows ERPs among 3 groups in LAA. The ERPs in HF rabbits at basic cycle lengths of 300, 250, and 200 ms were significantly longer compared with those in control rabbits. The ERPs in HF-RDN rabbits were significantly shorter compared with HF rabbits. APD<sub>90</sub> in HF rabbits was also significantly longer as compared with those in control and HF-RDN rabbits (Figure 3B and 3C). Inducibility of AF was significantly increased in HF rabbits compared with those in control rabbits, whereas decreased AF inducibility was observed in HF-RDN rabbits compared with those in HF rabbits as shown in Figure 3D.

### Protein Expression of Cleaved Caspase 3 and Tissue Fibrosis

To evaluate the apoptosis in LAA 4 weeks after MI, the protein of cleaved caspase 3 and caspase 3 was investigated among 4 groups. The ratios of cleaved caspase 3 to caspase 3 in HF rabbits and RDN sham rabbits (HF and open abdomen without RDN) were significantly higher than those in control and HF-RDN rabbits (Figure 4A and 4B). Those data were similar in HF rabbits and RDN sham rabbits.

To assess the progression of the fibrosis, LAA tissues were evaluated with Masson's trichrome staining as shown in Figure 5A through 5C. The degree of fibrosis in LAA was extensive in HF rabbits compared with that in control and HF-RDN rabbits. The degree of fibrosis significantly improved in HF-RDN rabbits compared with HF rabbits (Figure 5D).

### Immunohistochemistry Staining

To evaluate cardiac sympathetic nerves activity, tyrosine hydroxylase staining in LAA was performed. The percentage of the tyrosine hydroxylase-positive portions in LAA was significantly higher in HF rabbits compared with those of control and HF-RDN rabbits, respectively (Figure 6). In addition, to assess cytokine associated with the progression of fibrosis,

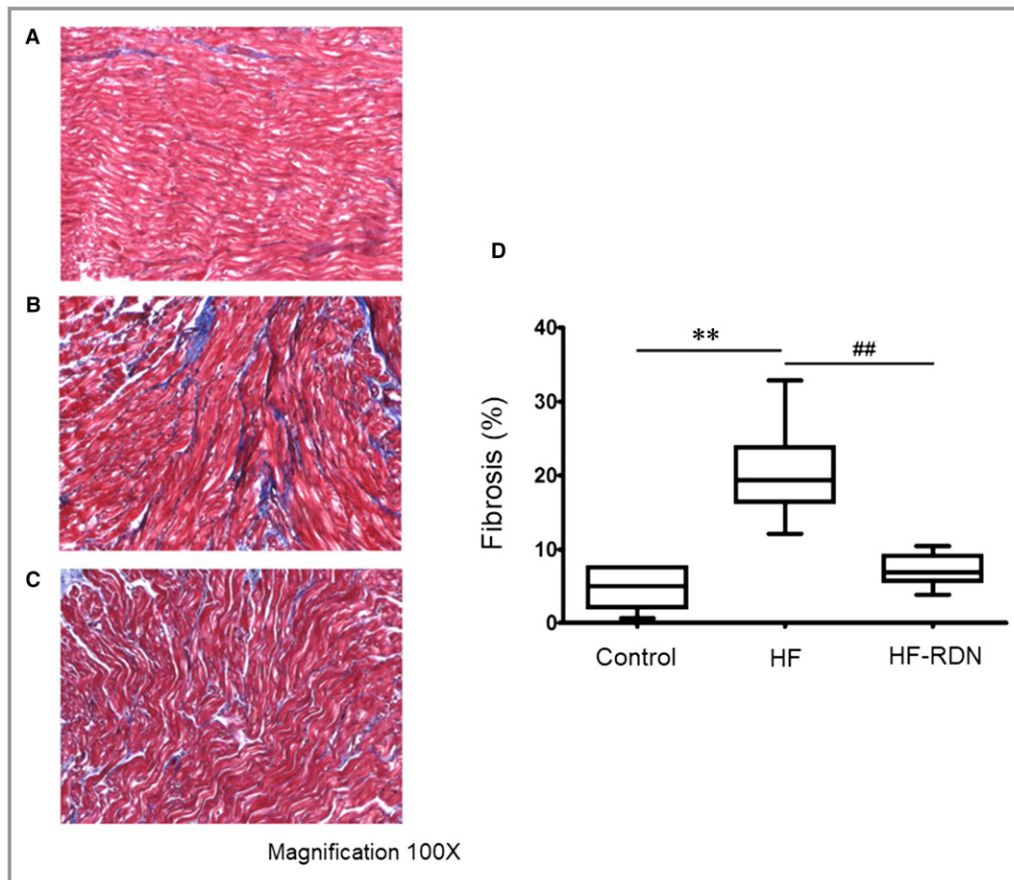


**Figure 5.** Atrial tissue fibrosis detected by Masson's trichrome staining in LAA. A, An example of atrial fibrosis in control rabbits. B, An example of atrial fibrosis in HF rabbits. C, An example of atrial fibrosis in HF-RDN rabbits. D, Quantitative analysis of fibrotic area in the LAA among all groups.  $**P < 0.01$  (vs control) and  $##P < 0.01$  (vs HF-RDN). The collagen area was calculated as a percentage of the total LAA area. HF indicates heart failure; LAA, left atrial appendage; RDN, renal denervation.

transforming growth factor- $\beta$  staining in LAA was also performed. The percentage of the transforming growth factor- $\beta$ -positive portions in LAA was significantly higher in HF rabbits compared with those of control and HF-RDN rabbits, respectively (Figure 7).

### Ionic Channel Expression

To determine the mechanism of ERP and APD shortened after RDN in our animal model, we investigated mRNA expression in various ion channels in the LAA samples by real-time-PCR (Figure 8). The mRNA levels of ion channels Cav1.2, Nav1.5, Kir2.1, and KvLQT1 decreased significantly in LAA of HF rabbits compared with those in control rabbits and HF-RDN rabbits.

### mRNA Levels of PI3K, AKT, and eNOS After RDN

We recently demonstrated that the PI3K/AKT/eNOS signaling pathway could play an important role in the regulation of atrial

arrhythmogenesis in ischemic HF models.<sup>6</sup> To investigate the mechanisms of RDN for the reverse structural and electrical remodeling, we evaluated the mRNA levels of PI3K, AKT, and eNOS in LAA. The mRNA levels of PI3K, AKT, and eNOS decreased significantly in HF rabbits compared with those in control rabbits and HF-RDN rabbits as shown in Figure 9.

## Discussion

### Major Findings

The progression of atrial remodeling, activation of the cardiac sympathetic nervous system, increase in renal catecholamine, and inducibility of AF in HF rabbits were dramatically suppressed by RDN. The impairment of the PI3K/AKT/eNOS signaling pathway may play a pivotal role in the development of atrial remodeling and the inducibility of AF in the ischemic HF model. RDN could regulate atrial arrhythmogenesis through the PI3K/AKT/eNOS signaling pathway.

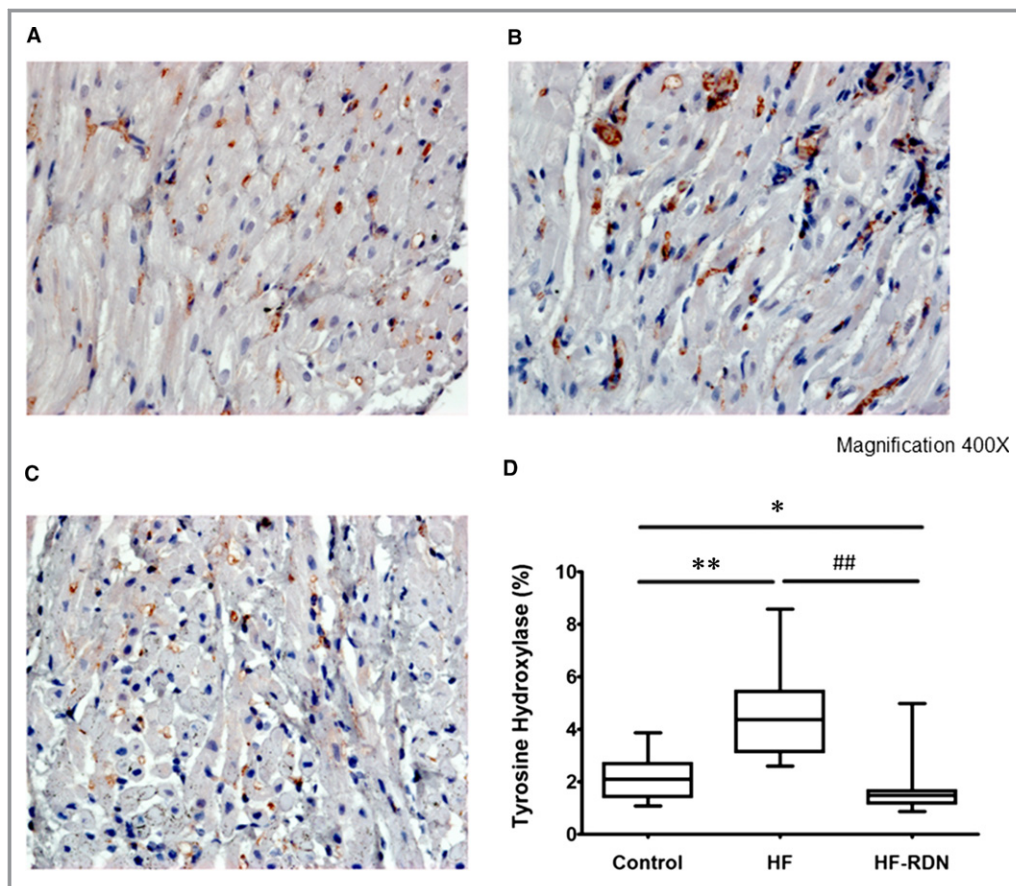


**Figure 6.** Immunohistochemistry staining of tyrosine hydroxylase in LAA. A, Control rabbits LAA. B, HF rabbits LAA. C, HF-RDN rabbits LAA. D, The percentage of the tyrosine hydroxylase–positive portions in LAA among 3 groups. \* $P < 0.05$  and \*\* $P < 0.01$  (vs control) and ### $P < 0.01$  (vs HF-RDN). HF indicates heart failure; LAA, left atrial appendage; RDN, renal denervation.

## HF Induced Atrial Remodeling

Cardiac remodeling after MI occurs progressively in the infarcted and noninfarcted myocardium, resulting in LV dilation and systolic dysfunction.<sup>1,2</sup> In addition, cardiac hypertrophy is induced as a compensatory process for damaged myocardium and preservation of cardiac function.<sup>18</sup> These ventricular remodelings lead to LA remodeling because the LA is a transporting chamber that receives blood from the pulmonary veins and conveys it to the ventricle. LA structural and electrical remodeling after MI, which is also characterized by the activation of sympathetic nervous and the circulating renin–angiotensin–aldosterone systems, finally contribute to the high inducibility of AF.<sup>19,20</sup> Furthermore, in HF status, sympathetic nervous and the circulating renin–angiotensin–aldosterone systems are further activated, resulting in the development of atrial arrhythmogenic substrates.<sup>13</sup> Given these facts, RDN may be dramatically effective for preventing the progression of atrial remodeling and the maintenance of AF in HF after MI because RDN can suppress the activation of sympathetic nervous and the circulating renin–angiotensin–

aldosterone systems.<sup>13</sup> Indeed, LV and LA dilatation, LV systolic dysfunction, and LV hypertrophy were observed in HF rabbits 4 weeks after coronary ligation, when compared with control rabbits. However, RDN could suppress the structural changes and AF inducibility. In the present study, both cardiac sympathetic nerves activity and the concentration of kidney tissue catecholamine in HF rabbits were significantly decreased by RDN. In HF, cardiac sympathetic activity is initially increased, and then renal sympathetic activity is increased.<sup>21</sup> In addition, it was previously demonstrated that the renal spillover of norepinephrine was significantly associated with the severity of HF and poor outcomes.<sup>22</sup> Therefore, RDN can attenuate the sympathetic hyperactivity in HF after MI.

## Effect of RDN on Atrial Remodeling in Ischemic HF

The effects of RDN on the atrial arrhythmogenic substrates in HF have not been fully clarified. Recently, we demonstrated that RDN might regulate the atrial arrhythmogenic substrates

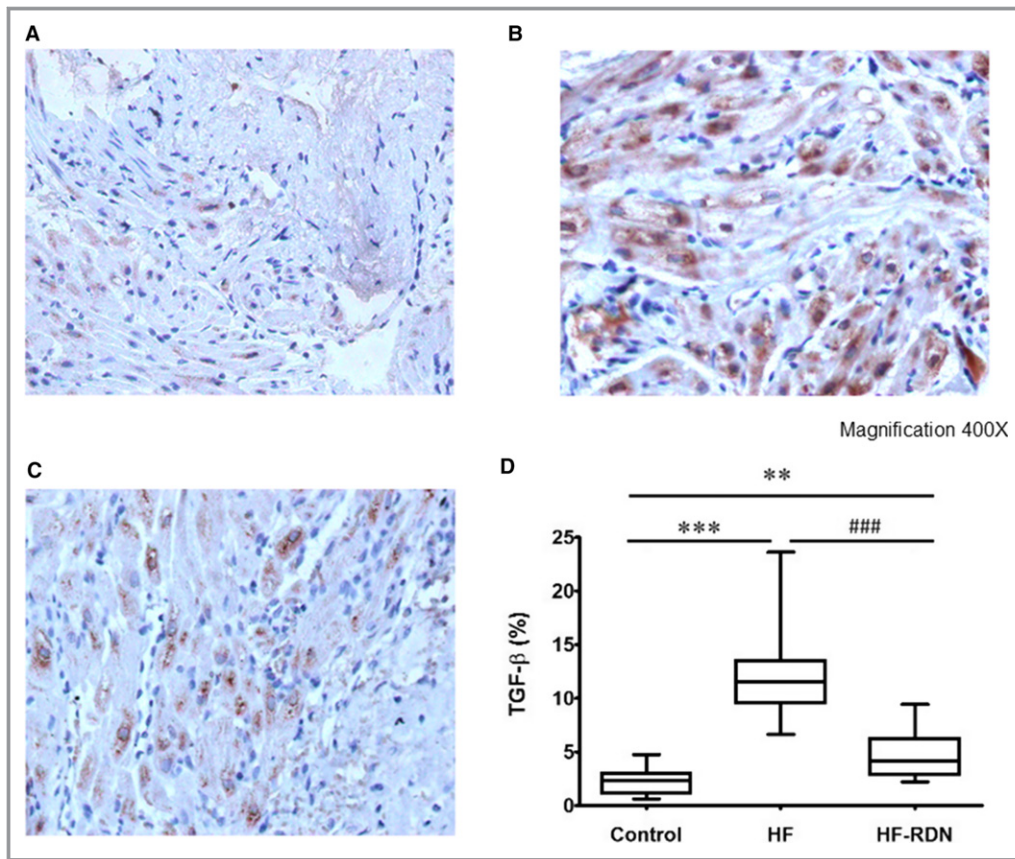


**Figure 7.** Immunohistochemistry staining of TGF- $\beta$  in LAA. A, Control rabbits LAA. B, HF rabbits LAA. C, HF-RDN rabbits LAA. D, The percentage of the TGF- $\beta$ -positive portions in LAA among 3 groups. \*\* $P$ <0.01 and \*\*\* $P$ <0.001 (vs control) and ### $P$ <0.001 (vs HF-RDN). HF indicates heart failure; LAA, left atrial appendage; RDN, renal denervation; TGF- $\beta$ , transforming growth factor- $\beta$ .

in HF rabbits paced for 4 weeks mostly through reverse structural remodeling.<sup>13</sup> However, in that study, ionic channel remodeling was not observed in pacing HF models. The severity of cardiac remodeling directly correlates with the rate and duration of pacing in pacing HF models,<sup>14</sup> whereas it has been shown that cardiac apoptosis occurs rapidly after MI, and sustained apoptosis is associated with the extent of cardiac remodeling in HF models after MI.<sup>23,24</sup> To evaluate the extent of cardiac apoptosis in the ischemic HF model, we evaluated the protein expression of cleaved caspase 3 and caspase 3, which are essential for the apoptotic process.<sup>25</sup> As a result, LAA in ischemic HF rabbits had a significantly higher activation of caspase 3 compared with that in control and HF-RDN rabbits. Therefore, ischemic HF rabbits might have atrial structural and electrical remodeling. In the present study, the extension of atrial fibrosis and structural remodeling in the ischemic HF model were significantly suppressed in HF-RDN rabbits, which is similar to our previous study.<sup>13</sup>

In order to evaluate the atrial ionic channel remodeling in HF, we analyzed the mRNA expressions of Cav1.2, Nav1.5, Kir2.1, and KvLQT1 in the LAA. The reduction of the L-type

calcium current (Cav1.2) and the potassium currents including Kir2.1 and KvLQT1 could induce atrial contractile dysfunction and arrhythmogenicity with electrical remodeling.<sup>26,27</sup> In addition, it was demonstrated that the reduction of sodium and potassium currents in HF might be responsible for APD prolongation.<sup>27</sup> In the present study, the mRNA expressions of Cav1.2, Nav1.5, Kir2.1, and KvLQT1 were significantly down-regulated in HF rabbits as compared with control rabbits. Therefore, the prolongation of ERPs and APD might be caused in HF rabbits. On the other hand, RDN could suppress the progression of ionic channel remodeling and shorten ERPs and APD in HF rabbits. These results suggest that RDN might regulate electrical remodeling in HF models after MI.

### RDN and PI3K/AKT/eNOS Signaling Pathway

The impairment of the PI3K/AKT/eNOS signaling pathway may lead to the progression of HF and the development of AF.<sup>6,28–32</sup> The inhibition of myocardial PI3K has the potential to induce cardiac dysfunction by decreasing cardiac contractility and increasing susceptibility to cardiac arrhythmias.<sup>28</sup> Loss of PI3K

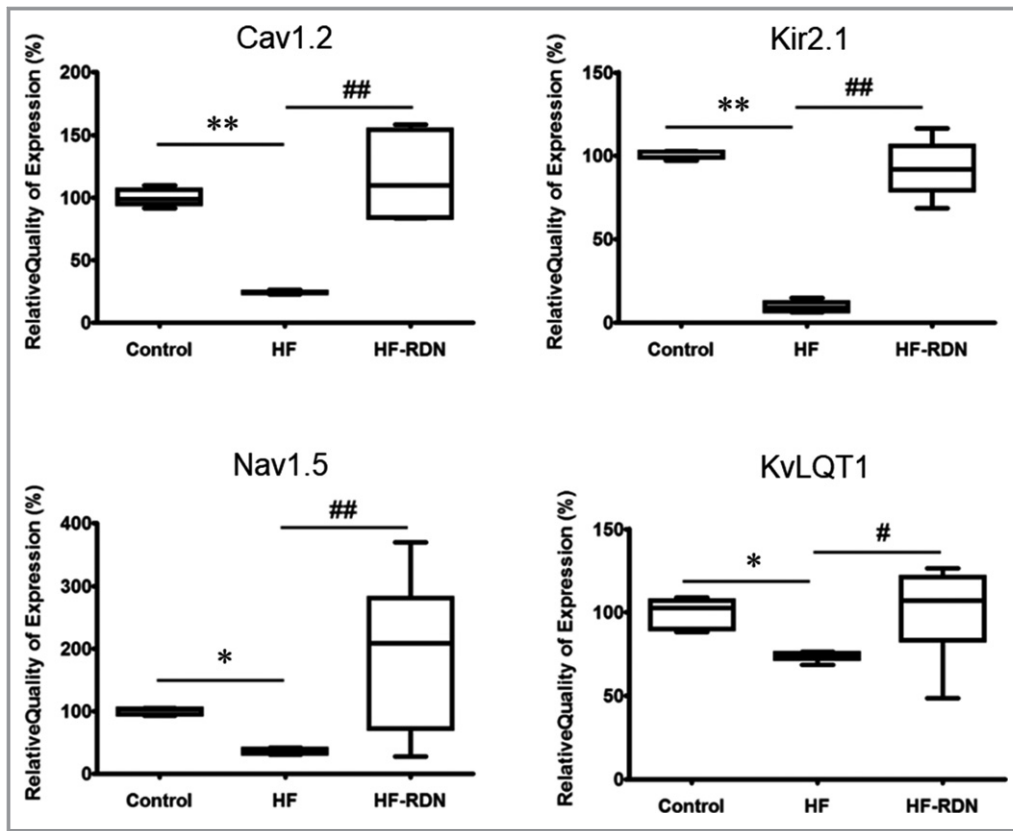


**Figure 8.** Expression of Cav1.2, Nav1.5, Kir2.1, and KvLQT1 in LAA. Messenger RNA expression of Cav1.2, Nav1.5, Kir2.1, and KvLQT1 as determined by real-time polymerase chain reaction. \* $P < 0.05$  and \*\* $P < 0.01$  (vs control), and # $P < 0.05$  and ## $P < 0.01$  (vs heart failure–renal denervation). HF indicates heart failure; LAA, left atrial appendage; RDN, renal denervation.

activity is associated with prolonged APD and QT intervals, whereas an increase in its activity markedly decreases atrial fibrosis.<sup>29,30</sup> Therefore, PI3K, a cardioprotective protein, is associated with the development of AF. Also, PI3K activates AKT through phosphatidylinositol 3-triphosphate, which inhibits apoptosis mediated by eNOS as the final messenger. AKT activates  $Ca^{2+}$ -activated  $K^+$  channels and may contribute to reduction in APD.<sup>31</sup> In addition, eNOS in the cardiomyocyte plays important roles for the maintenance of myocardial  $Ca^{2+}$  homeostasis, relaxation, and distensibility, as well as for protection from arrhythmia and abnormal stress stimuli.<sup>32</sup>

From this study, we found that downregulation of the PI3K/AKT/eNOS signaling pathway played an essential part in the progression of atrial structural and electrical remodeling. During HF, downregulation and desensitization of  $\beta$ -adrenoceptors may be associated with the impairment of the PI3K/AKT/eNOS signaling pathway.<sup>33</sup> On the other hand, it has been demonstrated that RDN blunted loss of  $\beta_1$ -adrenoceptor and  $\beta_2$ -adrenoceptor protein expression in HF models.<sup>34</sup> Therefore, the beneficial effect of RDN on cardiac remodeling may be related to prevention of the downregulation of the PI3K/AKT/eNOS signaling pathway.

## Clinical Implication

The beneficial myocardial effects of RDN were shown in the present study, whereas off-target effects of RDN (eg, post-procedural blood pressure reduction, worsening renal function, and vascular complication) were also reported previously.<sup>35,36</sup> Therefore, careful patient selection should be clinically considered in the application of RDN. The combination of AF and HF is associated with a higher risk of mortality.<sup>37</sup> For the management of AF patients with HF, medical therapy including  $\beta$ -blocker and amiodarone or radiofrequency catheter ablation is clinically considered, although therapeutic strategies for those patients have not been fully established. From our study, RDN might be an alternative therapeutic strategy in selected patients, particularly when medical therapy and radiofrequency catheter ablation have been ineffective or not tolerated.

## Limitation

There were several limitations in the present study. First, surgical and chemical RDN might have a different effect on

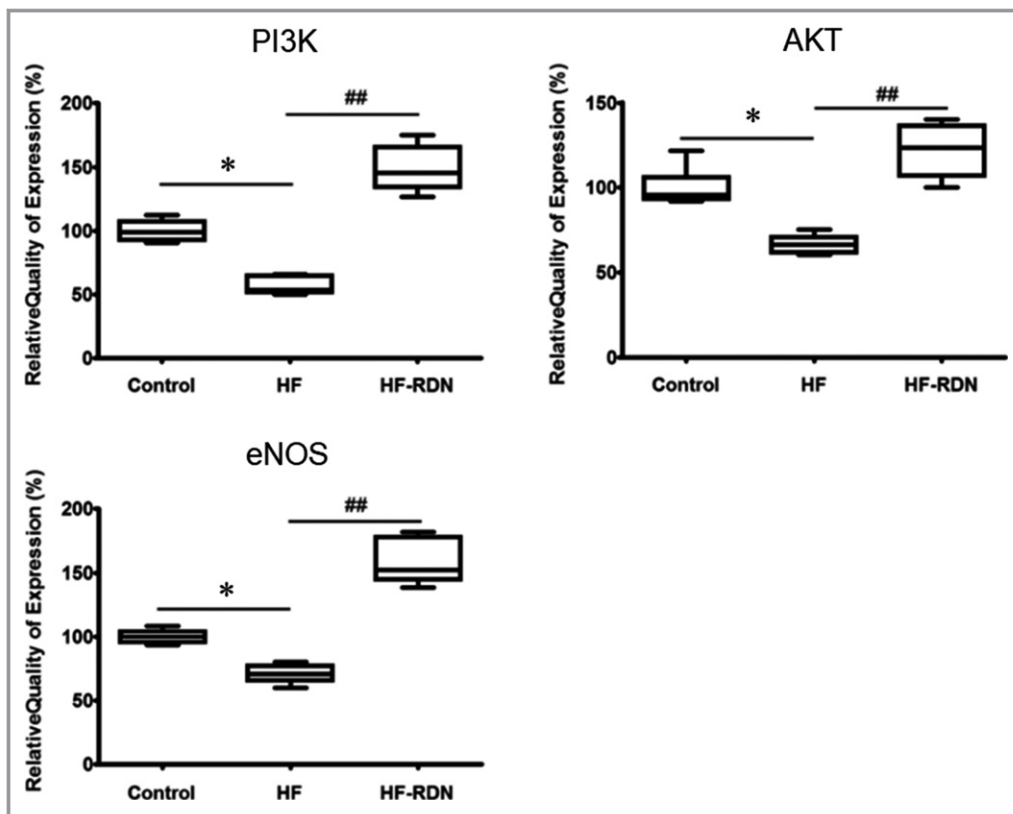


**Figure 9.** Expression of phosphoinositide 3-kinase (PI3K), AKT, and endothelial nitric oxide synthase (eNOS) in left atrial appendage. mRNA expression of PI3K, AKT, and eNOS as determined by real-time polymerase chain reaction. \* $P < 0.05$  (vs control), and  $^{##}P < 0.01$  (vs heart failure–renal denervation). HF indicates heart failure; RDN, renal denervation.

renal nerves, when compared with catheter-based RDN using a point-by-point radiofrequency catheter ablation as previously described.<sup>12,38</sup> However, we performed surgical and chemical RDN because the renal artery of the rabbit is too small. Second, there were no significant differences in the levels of plasma renin activity, renin, and aldosterone among the 3 groups. This may be explained by the fact that the renin–angiotensin–aldosterone system is regulated by complex feedback pathways in the HF model. We did not investigate the regulation of the renin–angiotensin–aldosterone system comprehensively in the present study. Finally, RDN has been demonstrated to attenuate sympathetic outflow via the central nervous system to the heart and other organs.<sup>9</sup> It has been reported that noninvasive methods of central sympathetic inhibition, such as clonidine, might have a cardioprotective effect.<sup>39</sup> Therefore, this noninvasive method may yield results similar to RDN. However, it has been considered that high doses of clonidine are required to regulate sympathetic activity and adverse effects (eg, sedation and dry mouth) will be commonly caused.<sup>39,40</sup> Therefore, the effect of RDN might be still better than that in drugs in terms of sympathetic inhibition.

## Conclusion

The ischemic HF model could induce atrial structural and electrical remodeling, resulting in high AF inducibility. RDN regulates atrial arrhythmogenesis through activation of the PI3K/AKT/eNOS signaling pathway, which may suppress AF in the failing heart after MI.

## Sources of Funding

This study was supported by Taipei Veterans General Hospital grant V104E7-002, V105C-121, V106C-056, Veterans General Hospitals University System (VGHUST)104-G7-3-2, VGHUST104-G7-3-2, VGHUST105-G7-9-2, Ministry of Science and Technology (MOST)104-2314-B-075-0, MOST104-2314-B-075-024-MY3, MOST 105-2314-B-075-036, and the foundation for the Development of Internal Medicine in Okinawa (grants 27-02-002).

## Disclosures

None.

## References

1. Yamani M, Massie BM. Congestive heart failure: insights from epidemiology, implications for treatment. *Mayo Clin Proc.* 1993;68:1214–1218.
2. Ho KKL, Anderson KM, Kannel WB, Grossman W, Levy D. Survival after the onset of congestive heart failure in Framingham Heart Study subjects. *Circulation.* 1993;88:107–115.
3. Schmitt J, Duray G, Gersh BJ, Hohnloser SH. Atrial fibrillation in acute myocardial infarction: a systematic review of the incidence, clinical features and prognostic implications. *Eur Heart J.* 2009;30:1038–1045.
4. Saczynski JS, McManus D, Zhou Z, Spencer F, Yarzelski J, Lessard D, Gore JM, Goldberg RJ. Trends in atrial fibrillation complicating acute myocardial infarction. *Am J Cardiol.* 2009;104:169–174.
5. Bhatia GS, Lip GY. Atrial fibrillation post-myocardial infarction: frequency, consequences, and management. *Curr Heart Fail Rep.* 2004;1:149–155.
6. Chong E, Chang SL, Hsiao YW, Singhal R, Liu SH, Leha T, Lin WY, Hsu CP, Chen YC, Chen YJ, Wu TJ, Higa S, Chen SA. Resveratrol, a red wine antioxidant, reduces atrial fibrillation susceptibility in the failing heart by PI3K/AKT/eNOS signaling pathway activation. *Heart Rhythm.* 2015;12:1046–1056.
7. Singhal R, Chang SL, Chong E, Hsiao YW, Liu SH, Tsai YN, Hsu CP, Lin YJ, Lo LW, Ha TL, Chen YC, Chen YJ, Chiou CW, Chen SA. Colchicine suppresses atrial fibrillation in failing heart. *Int J Cardiol.* 2014;176:651–660.
8. Liu SH, Hsiao YW, Chong E, Singhal R, Fong MC, Tsai YN, Hsu CP, Chen YC, Chen YJ, Chiou CW, Chiang SJ, Chang SL, Chen SA. Rhodiola inhibits atrial arrhythmogenesis in a heart failure model. *J Cardiovasc Electrophysiol.* 2016;27:1093–1101.
9. van Brussel PM, Lieve KV, de Winter RJ, Wilde AA. Cardiorenal axis and arrhythmias: will renal sympathetic denervation provide additive value to the therapeutic arsenal? *Heart Rhythm.* 2015;12:1080–1087.
10. Bhatt DL, Kandzari DE, O'Neill WW, D'Agostino R, Flack JM, Katzen BT, Leon MB, Liu M, Mauri L, Negoita M, Cohen SA, Oparil S, Rocha-Singh K, Townsend RR, Bakris GL; SYMPLICITY HTN-3 Investigators. A controlled trial of renal denervation for resistant hypertension. *N Engl J Med.* 2014;370:1393–1401.
11. Böhm M, Ewen S, Kindermann I, Linz D, Ukena C, Mahfoud F. Renal denervation and heart failure. *Eur J Heart Fail.* 2014;16:608–613.
12. Pokushalov E, Romanov A, Katritsis DG, Artyomenko S, Bayramova S, Losik D, Baranova V, Karaskov A, Steinberg JS. Renal denervation for improving outcomes of catheter ablation in patients with atrial fibrillation and hypertension: early experience. *Heart Rhythm.* 2014;11:1131–1138.
13. Yamada S, Lo LW, Chou YH, Lin WL, Chang SL, Lin YJ, Chen SA. Renal denervation regulates the atrial arrhythmogenic substrates through reverse structural remodeling in heart failure rabbit model. *Int J Cardiol.* 2017;235:105–113.
14. Hasenfuss G. Animal models of human cardiovascular disease, heart failure and hypertrophy. *Cardiovasc Res.* 1998;39:60–76.
15. Pye MP, Black M, Cobbe SM. Comparison of in vivo and in vitro haemodynamic function in experimental heart failure: use of echocardiography. *Cardiovasc Res.* 1996;31:873–881.
16. Linz D, Wirth K, Ukena C, Mahfoud F, Pöss J, Linz B, Böhm M, Neuberger HR. Renal denervation suppresses ventricular arrhythmias during acute ventricular ischemia in pigs. *Heart Rhythm.* 2013;10:1525–1530.
17. Devereux RB, Reichek N. Echocardiographic determination of left ventricular mass in man. Anatomic validation of the method. *Circulation.* 1977;55:613–618.
18. Rubin SA, Fishbein MC, Swan HJ. Compensatory hypertrophy in the heart after myocardial infarction in the rat. *J Am Coll Cardiol.* 1983;1:1435–1441.
19. Kettlewell S, Burton FL, Smith GL, Workman AJ. Chronic myocardial infarction promotes atrial action potential alternans, afterdepolarizations, and fibrillation. *Cardiovasc Res.* 2013;99:215–224.
20. Nattel S, Harada M. Atrial remodeling and atrial fibrillation: recent advances and translational perspectives. *J Am Coll Cardiol.* 2014;63:2335–2345.
21. Triposkiadis F, Karayannis G, Giamouzis G, Skoularigis J, Louridas G, Butler J. The sympathetic nervous system in heart failure physiology, pathophysiology, and clinical implications. *J Am Coll Cardiol.* 2009;54:1747–1762.
22. Petersson M, Friberg P, Eisenhofer G, Lambert G, Rundqvist B. Long-term outcome in relation to renal sympathetic activity in patients with chronic heart failure. *Eur Heart J.* 2005;26:906–913.
23. Backlund T, Palojoki E, Saraste A, Eriksson A, Finckenberg P, Kyto V, Lakkisto P, Mervaala E, Voipio-Pulkki LM, Laine M, Tikkanen I. Sustained cardiomyocyte apoptosis and left ventricular remodeling after myocardial infarction in experimental diabetes. *Diabetologia.* 2004;47:325–330.
24. Abbate A, Morales C, De Falco M, Fedele V, Biondi Zoccai GG, Santini D, Palleiro J, Vasaturo F, Scarpa S, Liuzzo G, Severino A, Baldi F, Crea F, Biasucci LM, Vetrotto GW, Gelpi RJ, Baldi A. Ischemia and apoptosis in an animal model of permanent infarct-related artery occlusion. *Int J Cardiol.* 2007;121:109–111.
25. Porter AG, Jänicke RU. Emerging roles of caspase-3 in apoptosis. *Cell Death Differ.* 1999;6:99–104.
26. Hu ST, Liu GS, Shen YF, Wang YL, Tang Y, Yang YJ. Defective Ca<sup>2+</sup> handling proteins regulation during heart failure. *Physiol Res.* 2011;60:27–37.
27. Nattel S, Maguy A, Le Bouter S, Yeh YH. Arrhythmogenic ion-channel remodeling in the heart: heart failure, myocardial infarction, and atrial fibrillation. *Physiol Rev.* 2007;87:425–456.
28. Ghigo A, Morello F, Perino A, Damilano F, Hirsch E. Specific PI3K isoform modulation in heart failure: lessons from transgenic mice. *Curr Heart Fail Rep.* 2011;8:168–175.
29. Pretorius L, Du XJ, Woodcock EA, Kiriazis H, Lin RC, Marasco S, Medcalf RL, Ming Z, Head GA, Tan JW, Cemerlang N, Sadoshima J, Shioi T, Izumo S, Lukoshkova EV, Dart AM, Jennings GL, McMullen JR. Reduced phosphoinositide 3-kinase (p110alpha) activation increases the susceptibility to atrial fibrillation. *Am J Pathol.* 2009;175:998–1009.
30. Lu Z, Wu CY, Jiang YP, Ballou LM, Clausen C, Cohen IS, Lin RZ. Suppression of phosphoinositide 3-kinase signaling and alteration of multiple ion currents in drug-induced long QT syndrome. *Sci Transl Med.* 2012;4:131ra150.
31. Cantley LC. The phosphoinositide 3-kinase pathway. *Science.* 2002;296:1655–1657.
32. Carnicer R, Crabtree MJ, Sivakumaran V, Casadei B, Kass DA. Nitric oxide synthases in heart failure. *Antioxid Redox Signal.* 2013;18:1078–1099.
33. Ghigo A, Laffargue M, Li M, Hirsch E. PI3K and calcium signaling in cardiovascular disease. *Circ Res.* 2017;121:282–292.
34. Zheng H, Liu X, Sharma NM, Patel KP. Renal denervation improves cardiac function in rats with chronic heart failure: effects on expression of  $\beta$ -adrenoceptors. *Am J Physiol Heart Circ Physiol.* 2016;311:H337–H346.
35. Böhm M, Mahfoud F, Ukena C, Hoppe UC, Narkiewicz K, Negoita M, Ruilope L, Schlaich MP, Schmieder RE, Whitbourn R, Williams B, Zeymer U, Zirkil A, Mancia G; GSR Investigators. First report of the Global SYMPLICITY Registry on the effect of renal artery denervation in patients with uncontrolled hypertension. *Hypertension.* 2015;65:766–774.
36. Krum H, Schlaich MP, Sobotka PA, Böhm M, Mahfoud F, Rocha-Singh K, Katholi R, Esler MD. Percutaneous renal denervation in patients with treatment-resistant hypertension: final 3-year report of the Symplicity HTN-1 study. *Lancet.* 2014;383:622–629.
37. Nieuwlaar R, Eurlings LW, Cleland JG, Cobbe SM, Vardas PE, Capucci A, López-Sendón JL, Meeder JG, Pinto YM, Crijns HJ. Atrial fibrillation and heart failure in clinical practice: reciprocal impact and combined management from the perspective of atrial fibrillation: results of the Euro Heart Survey on atrial fibrillation. *J Am Coll Cardiol.* 2009;53:1690–1698.
38. Pokushalov E, Romanov A, Corbucci G, Artyomenko S, Baranova V, Turov A, Shirokova N, Karaskov A, Mittal S, Steinberg JS. A randomized comparison of pulmonary vein isolation with versus without concomitant renal artery denervation in patients with refractory symptomatic atrial fibrillation and resistant hypertension. *J Am Coll Cardiol.* 2012;60:1163–1170.
39. Read MI, Harrison JC, Kerr DS, Sammut IA. Atenolol offers better protection than clonidine against cardiac injury in kainic acid-induced status epilepticus. *Br J Pharmacol.* 2015;172:4626–4638.
40. Hall JE, Uhrich TD, Ebert TJ. Sedative, analgesic and cognitive effects of clonidine infusions in humans. *Br J Anaesth.* 2001;86:5–11.